Available online at www.sciencedirect.com

SCIENCE DIRECT

Biochimica et Biophysica Acta 1668 (2005) 87–98

BIOCHIMICA ET BIOPHYSICA ACTA BBA

http://www.elsevier.com/locate/bba

Study of structure and orientation of mesentericin Y105, a bacteriocin from Gram-positive *Leuconostoc mesenteroides*, and its Trp-substituted analogues in phospholipid environments

Sabine Castano[a,*], Bernard Desbat[a], Antoine Delfour[b], Jean Marie Dumas[c], Alexandra da Silva[d], Jean Dufourcq[d]

[a]*Laboratoire de Physico-Chimie Moléculaire, Université de Bordeaux I, 351 cours de la Libération, 33405 Talence, France*
[b]*Institut J. Monod, Univ. Paris 7, place Jussieu, 75005 Paris, France*
[c]*I.B.M.I.G., Univ. Poitiers, Avenue du Recteur Pineau, 86022 Poitiers, France*
[d]*Centre de Recherche. Paul Pascal, CNRS, Avenue A. Schweitzer, 33600 Pessac, France*

Received 17 May 2004; received in revised form 16 November 2004; accepted 16 November 2004
Available online 2 December 2004

Abstract

Mesentericin Y105 (Mes-Y105) is a bacteriocin secreted by *Leuconostoc mesenteroides* which is particularly active on *Listeria*. It is constituted by 37 residues and reticulated by one disulfide bridge. It has two W residues, W18 and W37, which can be studied by fluorescence. Two single substituted W/F analogues were synthesized (Mes-Y105/W18 and Mes-Y105/W37) to differentiate the local environment around each W and to study their changes in the presence of lipid vesicles.

Fluorescence experiments show that, for the pure Trp-analogues, W18 and W37 are fully exposed to solvent whatever pH and buffer conditions. In the presence of lipid vesicles, both became buried. Lipid affinities were estimated: they are weak for zwitterionic phospholipids but an order of magnitude higher for negatively charged phosphatidylserine (PS) and phosphatidylglycerol (PG) lipids. On negatively charged PG lipids, Mes-Y105 and Mes-Y105/W37 display comparable lipid affinities. A decrease in lipid affinity is observed for Mes-Y105/W18 compared to Mes-Y105, which means that W37 would seem to be required for increased lipid selectivity. In the lipid-bound state W18 is strongly dehydrated, probably embedded into the acyl chains, while W37 stands more at the interface.

Mes-Y105 was also studied by polarization modulation infrared reflection absorption spectroscopy (PMIRRAS), alone and in various phospholipid environments, to obtain structural information and to assess lipid perturbations. At nanomolar concentrations close to those required for anti-Listeria activity, Mes-Y105 forms films at the air/water interface and inserts into negatively charged lipid monolayers. In situ infrared data show that Mes-Y105 binding only affects the polar head group vibrations while the lipid order of the acyl chains remains unaffected. The PMIRRAS show that Mes-Y105 folds into an N-terminal antiparallel β-sheet followed by an α-helix, both structures being tilted (40°) compared to the normal at the interface, which is in agreement with the thickness estimated by Brewster angle microscopy (BAM). All these data support the proposal of a new model for Mes-Y105 at the membrane interface.

Keywords: Mesentericin; Bacteriocin; Lipid-bound structure; Peptide orientation; Fluorescence; PMIRRAS

Abbreviations: Mes-Y105, mesentericin; POPC, palmitoyl-oleyl-phosphatidylcholine; PS, phosphatidylserine; DMPC, dimyristoyl-phosphatidylcholine; EPC, egg phosphatidylcholine; DMPG, dimyristoyl-phosphatidylglycerol; DPPG, dipalmitoyl-phosphatidylglycerol; TFE, trifluoroethanol; PMIRRAS, polarization modulation infrared reflection absorption spectroscopy; BAM, Brewster angle microspopy; CD, circular dichroïsm; FRET, fluorescence resonance energy transfer

* Corresponding author. Tel.: +33 5 40 00 63 64; fax: +33 5 40 00 66 45.
E-mail address: s.castano@lpcm.u-bordeaux1.fr (S. Castano).

0005-2736/$ - see front matter © 2004 Elsevier B.V. All rights reserved.
doi:10.1016/j.bbamem.2004.11.008

1. Introduction

Mesentericin Y105 (Mes-Y105) is a class IIa bacteriocin [1] from *Leuconostoc mesenteroides*, a gram-positive bacteria. Mes-Y105 is constituted by 37 residues and is reticulated by one disulfide bridge between residues C_9 and C_{14}. Its sequence is the following: KYYGNGVHCTKSGCSV-NW_{18}GEAASAGIHRLANGGNGFW_{37} [2]. Mes-Y105 is efficient and quite selective antibacterial peptide acting particularly on *Listeria monocytogenes* down to the nanomolar concentration range. It is able to severely decrease the membrane potential of the target cells, but it also modifies many transport systems [3,4]. The first Mes-Y105 structure–function relationships were proposed after purification [5]. In contrast to other nonspecific lytic peptides, where numerous sequence changes and deletions can still maintain biological activity, the complete peptide length and the integrity of the single disulfide bridge are mandatory for Mes-Y105 activity. From CD data of Mes-Y105 in buffer solution and comparison with other antimicrobial peptides, a structure was proposed with an N-terminal capable of involvement in interaction with a putative receptor while a characteristic amphipathic α-helix from residues 17 to 31 would allow lipid binding to the membrane [5]. Several toxins closely related to Mes-Y105 were studied by fluorescence to characterize their interactions with phospholipids [6,7] and by NMR to propose structures for leucocin A and carnobacteriocin B2 in buffer solution, in the presence of TFE, and in detergent micelles [8–10]. Currently, several models for accounting membrane interactions and cytotoxicity are proposed, while there are still contradictory structural changes and different mechanisms for toxin-induced membrane permeabilization [11–14].

Most of the class IIa bacteriocins have several W residues which allow the monitoring of the toxin behavior by fluorescence. Mes-Y105 has two W residues at positions 18 and 37. Single substitution analogues of one of them will allow selective monitoring of the behavior of each one. W18 is almost invariant for class IIa bacteriocins [1]; it was suggested that it is involved in an amphipathic α-helix. W37 is mandatory for activity [5]. Herein for the first time, the intrinsic fluorescence of Mes-Y105 has been used to monitor the behavior of three different synthetic peptides in solution and in the presence of phospholipid vesicles: (i) Mes-Y105, which has the natural toxin sequence and then fluorescent W18 and W37 residues, (ii) Mes-Y105/W37, which only differs by the W18→F substitution, and (iii) Mes-Y105/W18 with the single W37→F substitution.

In a second step, the tensio-active behavior of Mes-Y105 and its interactions with phospholipid monolayers have been studied in the very low concentration range where it displays activity on cells. Finally the structure and the orientation of the toxin have been documented using polarization modulation infrared reflection absorption spectroscopy (PMIRRAS), a specific IR technique which makes it possible to obtain spectra of both peptides and their mixtures with lipids in situ at the air/water interface [15].

2. Materials and methods

2.1. Peptide synthesis

Peptides were synthesized by a standard 9-fluorenylmethoxycarbonyl (Fmoc)-based solid-phase method [16], using an automated synthesizer (Applied Biosystems, model 433A). The *N*α-Fmoc-amino acids were coupled to the growing peptide chain using a solution in *N*-methylpyrrolidone with 1-hydroxybenzotriazole (HOBt)-2-(1*H*-benzotriazol-1-yl-1,1,3,3-tetramethyluronium hexafluorophosphate (HBTU) in *N*,*N*-dimethylformamide. All these reagents were from Novabiochem (France); other solvents and reagents used in peptide synthesis were obtained from SDS and Sigma.

Side-chain protections were as follows: *tert*-butyloxycarbonyl for lysine; pentamethyl-bihydrobenzofuran-5-sulfonyl for arginine; *O*-*tert*-butyl ester for glutamic acid; *O*-*tert*-butyl ether for serine, threonine and tyrosine; trityl for asparagine, cysteine and histidine.

Peptide–resin cleavage and side chain deprotection reactions were carried out in reagent K [17]. After filtering to remove the resin followed by ether precipitation at low temperature, the crude peptides were recovered after centrifugation, dissolved in 20% acetic acid and lyophilized.

Then peptides were purified by preparative reverse-phase HPLC on a Waters RCM compact preparative cartridge Deltapak C-18. Homogeneity of the peptides was assessed by analytical HPLC on a Lichrospher ODS 2 column and the purified peptides were characterized by electro-spray mass spectrometry (Applied Biosystems EP165).

The magainin analogue used herein as standard for PMIRRAS experiments corresponds to magainin 2 with Lys substitution. It was also obtained by solid state synthesis as already explained [18]. It was kindly provided by Dr. O. Siffert.

Peptide concentrations were estimated from the UV absorption spectra of stock solutions (2 mM) in methanol using ε_{280}=5600 M^{-1} cm^{-1} and ε_{280}=1000 M^{-1} cm^{-1} for W and Y, respectively.

2.2. HPLC analysis

The retention times of the peptides eluted in a CH_3CN/water gradient were measured by RP-HPLC on a C_{18} reverse phase Purospher RP-18 end-capped semi-preparative column (125×4 nm, 5 μm particle size), in conjunction with a Waters millenium HPLC system as previously described [19].

2.3. Lipids vesicles

EPC was purified in the laboratory; PS and PG were from Lipid Products (Nutfield, UK); synthetic lipids POPC, DMPC, DMPG and DPPG were from Avanti Polar Lipids (Birmingham, AL, USA).

For monolayer studies concentrated chloroform solutions were prepared. For vesicle preparation, lipids were first dried under vacuum, and/or lyophilized. Then they were hydrated by the buffer used in experiments, degassed under N_2 and tip sonicated for a few minutes to get essentially single unilamellar vesicles (SUVs) as already checked by different methods [20].

2.4. Fluorescence spectroscopy and lipid binding constant analysis

Fluorescence measurements were performed on a Spex Fluoromax spectrometer at 25 °C, generally on excitation at 280 nm with 4-nm band pass. The emission spectra were always subtracted from that of blanks, i.e., buffer with the same final amount of lipids. Peptide solutions at 2 μM in Tris 20 mM buffer pH 7.5 were made up by dilution of a few milliliters of stock solution in MeOH. Lipid interactions were performed in situ on the fluorescence cuvette increasing the lipid to peptide molar ratio, Ri, by successive dropwise additions of concentrated SUV suspensions (6.25 mM in lipids). Buffer at pH=4.5 was obtained by decreasing the pH of the Tris 20 mM buffer pH 7.5 by progressive additions of HCl.

The binding constants of Mes-Y105 for lipid vesicles can be estimated from the changes of the spectra maximum emission wavelength (λ_{max}) curves analyzed using the following equation [7,21]:

$$\varepsilon - 1 = (\varepsilon_b - 1) - (K_d/n)(\varepsilon - 1)/m \quad (1)$$

where K_d, n and m are the dissociation constant of a lipid–peptide complex, the number of binding sites per lipid, and the total lipid concentration, respectively. The relative blue shift is defined as $\varepsilon = \lambda_{max}^0/\lambda_{max}$, λ_{max}^0 denoting the maximum emission wavelength in the absence of lipids, while ε_b is the maximal value obtained when all the peptide is bound to lipid vesicles. The slope of the linear plots of $(\varepsilon-1) = f((\varepsilon-1)/m)$ gives the K_d/n values.

2.5. Film formation and surface pressure measurements

Monolayer experiments were performed on a computer-controlled Langmuir film balance (Nima Technology, Coventry, England). The rectangular trough (V=110 cm^3, S=145 cm^2) and the barrier were made of Teflon. The surface pressure (Π) was measured by the Wilhelmy method using a filter paper plate. The trough was filled with an aqueous buffer (20 mM Tris, HCl, pH=7.5) using ultra pure water (Milli-Q, Millipore). The experiments were carried out at 25±2 °C. A few microliters of MeOH peptide stock solutions were injected into the subphase to define the total Mes-Y105 concentration. Mixed peptide/lipid films were obtained as previously described [22]. In short, the pure lipid was spread first at the air/water interface from chloroform solutions, then after ≈15 min the phospholipid film was slowly compressed up to 30 mN/m. In a second step, a few microliters of concentrated peptide solutions were injected into the subphase.

2.6. PMIRRAS spectroscopy

PMIRRAS spectra were recorded on a Nicolet 740 spectrometer equipped with a photovoltaic HgCdTe detector cooled at 77 K. Generally, 200 or 300 scans were co-added at a resolution of 4 or 8 cm^{-1} for pure peptide or mixed peptide/DMPC monolayers, respectively. In short, PMIRRAS combines FT-IR reflection spectroscopy with fast polarization modulation of the incident beam between parallel (p) and perpendicular (s) polarization. Two-channel processing of the detected signal makes it possible to obtain the differential reflectivity spectrum:

$$\Delta R/R = (\mathrm{Rp} - \mathrm{Rs})/(\mathrm{Rp} + \mathrm{Rs})J_2.$$

To remove the contribution of liquid water absorption and the dependence on Bessel functions J_2, the monolayer spectra are divided by that of the subphase. With an incidence angle of 75°, transition moments preferentially oriented in the plane of the interface give intense and upward oriented bands, while perpendicular ones give weaker and downward oriented bands [23].

The decomposition of the amide I and amide II spectral region (1500–1800 cm^{-1}) into individual bands was performed with the Peaksolve (version 3.0, Galactic) software and analyzed as a sum of Gaussian/Lorentzian curves, with consecutive optimization of amplitudes, band positions, half-width and Gaussian/Lorentzian composition of the individual bands.

2.7. Brewster angle microscopy (BAM) measurements

The morphology of mixed mesentericin/DPPG layers at the air/water interface was observed using a Brewster angle microscope (NFT BAM*2plus*, Göttingen, Germany) mounted on the glass Langmuir trough. The microscope was equipped with a frequency doubled Nd:Yag laser (532 nm, 20 mW), polarizer, analyser and a CCD camera. The spatial resolution of the BAM was about 2 μm, and the image size 625×400 μm.

3. Results

3.1. Intrinsic fluorescence study and HPLC analysis of mesentericin Y105 and its analogues

3.1.1. Peptides free in solution

The emission spectrum of natural Mes-Y105 is centered at about 351 nm. Single W analogues, namely Mes-Y105/W18 and Mes-Y105/W37, gave rather similar spectra with weakly different maximum emission positions: 354±2 and 347±2 nm for Mes-Y105/W18 and Mes-Y105/W37, respectively (Fig. 1a). In buffer at pH 7.5, the emission

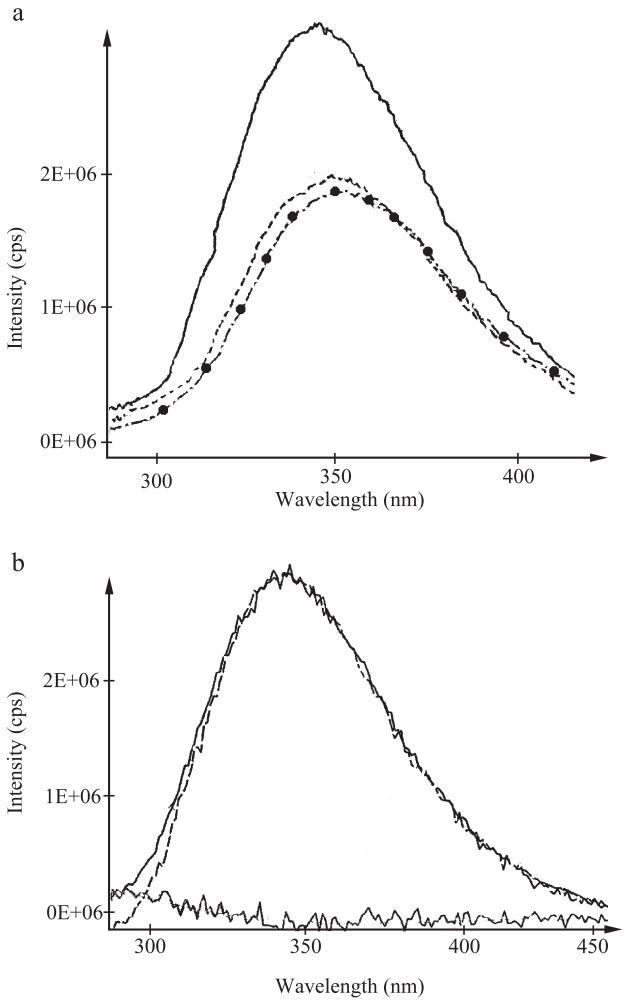

Fig. 1. Fluorescence emission spectra of mesentericin and its analogues (a) on excitation at λ_{exc}=280 nm of Mes-Y105 (—), Mes-Y105/W18 (- - -) and Mes-Y105/W37 (-●-). (b) Fluorescence emission spectra of Mes-Y105/W18 normalized at λ>350 nm; λ_{exc}=280 nm (—); λ_{exc}=295 nm (- - -); lower trace (—) difference spectrum reflecting Y contribution when λ_{exc}=280 nm. Tris 20 mM, pH 7.5 buffer, [peptide]=2 μM.

intensities of both single W containing analogues are about similar and half that of the total emission intensity of the Mes-Y105 peptide. On excitation at 295 nm, which essentially abolishes the Y excitation and allows the recovery of the only W emission, there is no significant shape change of the normalized spectra. The Y contribution on excitation at 280 nm is then estimated by difference and is very weak and only detectable near 300 nm (Fig. 1b). Then, on excitation at 280 nm, one can consider that Mes-Y105 behaves in solution as having essentially two independent emitting residues W18 and W37 both being almost fully accessible to buffer. The higher wavelength for the emission maximum for W37 can be attributed to its proximity to the ionized CO terminal of the peptide [24]. The lack of significant contribution from Y2 and Y3 could be due to their quenching probably by amine groups of the K and NH_2 terminal group or to Y→W resonance energy transfer (FRET). However, on dual excitation (280/295 nm) the ratios of the quantum yields are the same for Mes-Y105, Mes-Y105 analogues and melittin, used as a reference since it has a single W and lacks Y. Contribution of intramolecular FRET to Mes-Y105 fluorescence properties can then be discarded.

3.1.2. HPLC analysis of Mes-Y105

It has been suggested that the affinity for C_{18} chains on reverse phase HPLC reflects the ability of a peptide to interact with membrane and generally parallels the cytotoxic activity [25]. When eluted in a CH_3CN/water gradient, the retention time, RT, of Mes-Y105 is very short, 1.2 min, similar to that of the shortest cytolytic pentapeptide KLLLK already studied and that of a random non-amphipathic LK15 peptide [26]. This is significantly shorter than those of magainin analogue or melittin used as reference with RT values of 3.3 and 5.0 min, respectively. This fits in neatly with the classic correlation between RT and the very weak hydrophobic moment for the whole Mes-Y105 peptide

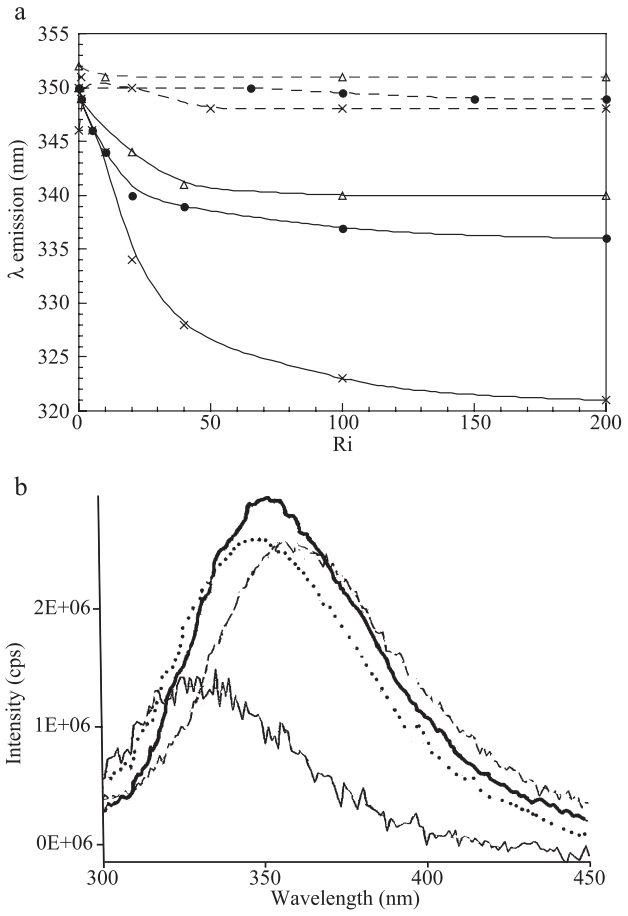

Fig. 2. Fluorescence of Mes-Y105, Mes-Y105/W18 and Mes-Y105/W37 bound to EPC and PS vesicles. (a) Changes in the maximum emission wavelengths ($\lambda_{max,em}$) versus Ri (- - - -) interaction with EPC vesicles; (—) interaction with PS vesicles Mes-Y105 (●); Mes-Y105/W18 (×); Mes-Y105/W37 (△). (b) Fluorescence emission spectra of Mes-Y105/W37 (- - - -) and Mes-Y105/W18 (▬) free and Mes-Y105/W37 (• • • •) and Mes-Y105/W18 (—) bound to PS vesicles. Tris 20 mM, pH 7.5 buffer, [peptide]=2 μM.

when assumed to be in helical structure (μ_{total}=3.6; $(\mu)_{res}$=0.1).

3.1.3. Peptides in the presence of phospholipids vesicles

When vesicles are added to peptide solutions, different changes are observed according to the net charge of the phospholipids. On adding zwitterionic EPC vesicles, very limited and progressive changes are observed for all the peptides (Fig. 2a). Even increasing the lipid to peptide molar ratio, Ri, up to 800–1000 leads to relatively modest blue shifts of the emission maxima (Table 1), from 6 nm for the natural peptide and Mes-Y105/W18 up to 8–9 nm for the W37 analogue. Concomitantly weak and very progressive intensity changes are detected. This can be interpreted as a weak partitioning of the peptides into this zwitterionic lipid. As a further experiment, when calcein was trapped into EPC LUVs, dropwise addition of Mes-Y105 up to Ri=1 fails to induce any significant leakage of the trapped dye (data not shown).

On the contrary, on adding negatively charged phospholipid vesicles composed of PS, drastic changes occur on the emission spectra of Mes-Y105 and its analogues, even at lower lipid to peptide molar ratio (Ri < 50) (Fig. 2a and b). For Mes-Y105/W18, the emission maximum shifts down to 321 nm with a strong quenching; for the Mes-Y105, it shifts to 336 nm; and for Mes-Y105/W37, it only shifts to 340 nm at Ri=100. The very large 26-nm blue shift of W18 emission indicates an apolar medium around this residue probably at contact of the lipid chains; the weaker change by 14 nm of W37 corresponds probably to an interfacial location of this last residue. Similar data were obtained using PG as negatively charged lipid. In this case the changes in spectra are ended at very weak values, Ri<10. The maximal blue shifts for totally bound peptides are rather similar to those observed for PS and with the same hierarchy (Table 1).

3.1.4. pH and ionic strength effects

Since interactions are quite sensitive to the lipid's net charge, one can wonder what happens on changing the peptide net charge. Mes-Y105 contains various charged groups which can be protonated by lowering the pH below 6: two H residues, at positions 8 and 27, a single E_{20} residue and free N and C terminal groups of which ionization state can change on lowering the pH. Considering the bulk pK_a values for α-COOH, α-NH_3^+, K, H, and E, 3.5, 7.5, 10.4, 6.5 and 4.25, respectively [30], one can therefore expect an increase of the net charge from +2 to +4 on decreasing the pH from 7.5 to 4.5.

Such a pH change has no effect on the emission maximum wavelengths of pure peptides in solution which remain centered at the same position (Table 1), while a strong quenching occurs in acidic medium and remains constant from pH 6 to 4.5.

The effect of Mes-Y105 charge changes on interaction with lipids was investigated using PG vesicles since their net charge remains constant in the studied pH range. Decreasing pH results in steeper slopes of the changes in emission maximum wavelengths induced by lipid addition, the plateau values are obtained at lower Ri values and the final blue shift is larger at pH=4.5 (−21 nm) compared to that measured at pH 7.5 (−14 nm) (Fig. 3a). This can be interpreted as an increased affinity and a more severe dehydration of W's on lowering the pH.

Another relevant experiment to document electrostatic dominant interactions is to look at its dependence on ionic strength. Addition of 150 mM NaCl significantly flattened the changes in λ_{max}, and finally in 1.7M NaCl there is no

Table 1
Changes in the maximum emission wavelength (nm) of Mes-Y105, Mes-Y105/W18 and Mes-Y105/W37 alone and in the presence of different lipids excess, and binding constants, K_d/n (μM), in different pH and ionic strength conditions

	Free peptides		Peptides bound to lipids (Ri=200)			
	pH=7.5	pH=4.5	EPC (pH=7.5)	PS (pH=7.5)	PG (pH=7.5)	PG (pH=4.5)
Mes-Y105						
$\lambda_{max,em}$	350	350	344	337	340	329
$\Delta\lambda$			−6	−13	−10	−21
K_d/n			217	13	4 (28^+)	2 (14^+)
Mes-Y105/W18						
$\lambda_{max,em}$	346	346	340	322	326	nd
$\Delta\lambda$			−6	−24	−20	
K_d/n			75	43	nd	
Mes-Y105/W37						
$\lambda_{max,em}$	354	352	345	340	342	nd
$\Delta\lambda$			−9	−14	−12	
K_d/n			278	13	nd	
Melittin [27]	349	nd	335	331	331	nd
Magainin [28,29]	352	nd	nd	nd	336	nd
Pediocin PA-1 [6,7]	353	nd	353		333	

(+) Plus 150 mM NaCl; nd: not determined.
Fluorescence parameters of melittin and magainin were chosen as standards since these peptides display a single W in their sequence and a strong antimicrobial activity. Pediocin PA, like Mes-Y105, belongs to the class IIa bacteriocins.

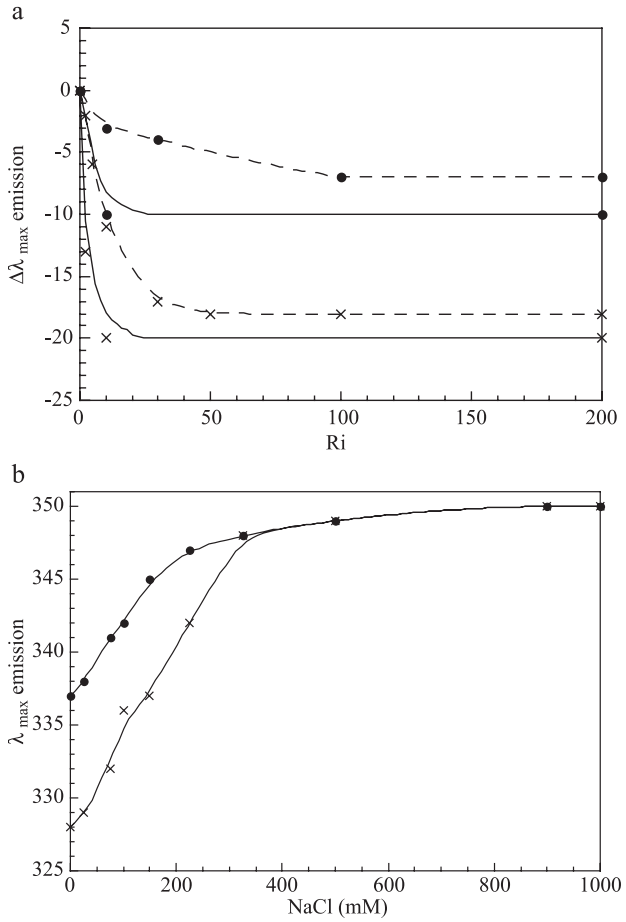

Fig. 3. pH and ionic strength changes induced on Mes-Y105 interaction with PG vesicles. (a) Maximum emission wavelengths ($\lambda_{max,em}$) variations versus Ri×pH=4.5; (●) pH=7.5, without NaCl (—); NaCl 150 mM (- - - -). (b) Effect of ionic strength on the maximum emission wavelength ($\lambda_{max,em}$) of Mes-Y105 previously bound to PG vesicles. (–●–) pH=7.5, Ri=30; (–×–) pH=4.5, Ri=56, [peptide]=2 μM.

longer any detectable shift (Fig. 3a). Conversely, if Mes-Y105 is first completely bound to lipid vesicles at low ionic strength (20 mM) before increasing ionic strength by successive NaCl additions, an immediate and progressive red shift of λ_{max} is observed. This results in the total recovery of the spectra of free peptides for NaCl>400 mM, whatever the pH of the experiment (Fig. 3b). Therefore, the lipid binding of Mes-Y105 is essentially charge-dependent, totally reversible by moderate ionic strength. This means that the toxin can be easily released or expelled from the interface.

3.1.5. Peptide–lipid affinity

The changes in the fluorescence parameters (Figs. 2 and 3) allow the estimation of the relative dissociation constant K_d/n (where n is the number of binding sites per lipid molecule) applying Eq. (1) and using classic approaches and approximations [7,21]. The affinities of Mes-Y105 and its analogues calculated for different lipids in various conditions vary strongly as shown on Table 1.

The smallest K_d/n values, in the nanomolar range, indicate a strong affinity of Mes-Y105 for the charged lipid membranes. At pH=7.5, Mes-Y105 affinity for zwitterionic EPC vesicles is much weaker than for negatively charged PS and PG ones. The ratio of these two values compared to that for EPC gives a selectivity ratio for the charged lipids of about ≈20-fold and 55-fold, respectively. At low pH, the increase of the Mes-Y105 net charge is paralleled by a twofold increase of the affinity for PG. Conversely, increasing the ionic strength up to 150 mM results in a sevenfold decrease of Mes-Y105 affinity for PG vesicles whatever the pH.

The Mes-Y105 analogues also have lipid selectivity, their K_d/n values are also stronger for anionic PS vesicles than for zwitterionic EPC ones. For Mes-Y105/W37, the K_d/n values and a selectivity ratio ≈20 were identical to those of Mes-Y105. For Mes-Y105/W18 reverse changes of K_d/n for PC and PG were observed; this led to a significant decrease from 20 to 2 of the selectivity factor. The comparable affinities measured for Mes-Y105/W37 and Mes-Y105 in the same conditions provide evidence for the conclusion that W18→F substitution has no influence on the peptide/lipids interactions. However, the different K_d/n obtained for Mes-Y105/W18 compared to Mes-Y105 show that the W37→F substitution changes lipid affinities and selectivity, and, thus, that W37 plays a specific role at the membrane interface.

3.2. Surface activity, structure and orientation of mesentericin studied by PMIRRAS

3.2.1. Behavior of Mes-Y105 free in solution

When Mes-Y105 in solution is introduced in the buffer subphase of a Langmuir trough in the concentration range of some tens of nanomolar, the peptide significantly decreases the surface tension of buffer. The peptide film can be compressed, and the surface pressure increases smoothly up to 20 mN/m (Fig. 4). In similar experimental conditions, a magainin analogue or a strongly lytic ideally amphipathic LK15 compound (sequence KLLKLLLKLLLKLLK) [22] yields films which are more stable, up to 30 to 35 mN, respectively.

The in situ PMIRRAS spectra at the air/water interface of Mes-Y105 films compressed at 10 and 20 mN/m display well-resolved but quite broad amide bands (Fig. 5). The complex amide I domain is centered at ≈1652 cm^{-1}, with shoulders around 1635/1695 and 1675 cm^{-1}, corresponding respectively to α-helix, antiparallel β-sheets and β-turns [31–34]. A broad and relatively intense amide II band is centered at 1530 cm^{-1}. The global shape of the amide I domain of pure Mes-Y105 remains unchanged when the lateral pressure is increased from 10 to 20 mN/m, which means that the global secondary structure of Mes-Y105 is pressure-independent. This compression from 10 to 20 mN/m, which results in a twofold decrease in total film area, i.e., a twofold higher peptide density in the IR

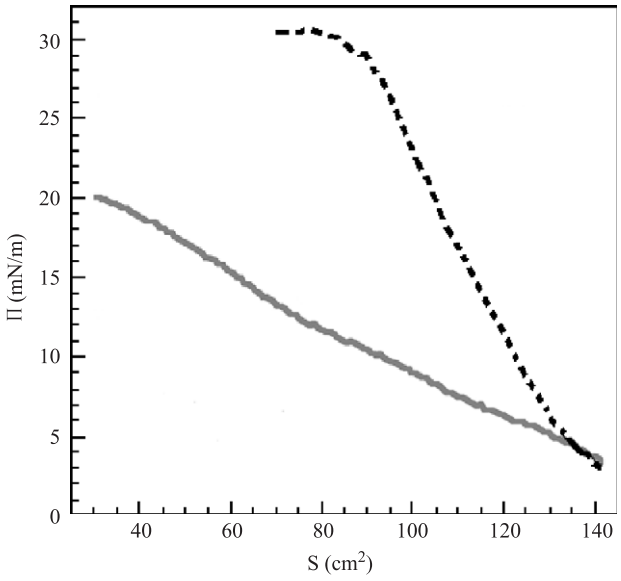

Fig. 4. Compression isotherms on a Langmuir trough of the cytotoxic peptides. (—) Mesentericin (Mes-Y105); (- - - -) Magainin. Subphase: [peptide]=36 nM, 20 mM Tris buffer, HCl, pH=7.5; T=23 °C.

beam, should result in a global intensity increase. However, during this process (Fig. 5), the amide I/amide II ratio increases as well as the 1695 cm^{-1} amide I contribution of antiparallel β-sheet. This suggests a progressive but slight reorientation of the antiparallel β-sheets during the compression from a tilted (≈45°) to a flatter orientation (≈25°) [22,35,36]. Magainin analogue and ia-LK15 used as standards display a narrow amide I band centered at 1655 cm^{-1} and a high amide I/amide II band intensity ratio, both characteristic of pure α-helical structures with their long axis essentially parallel to the interface plane [22,35,37].

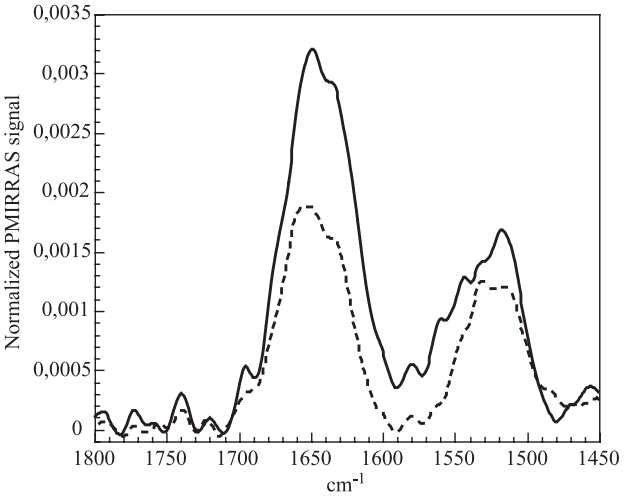

Fig. 5. PMIRRAS spectra of Mes-Y105 at the air/water interface. (- - -) Π=10 mN/m; (—) Π=20 mN/m. Subphase: 20 mM Tris buffer, HCl, pH=7.5; T=23 °C.

3.2.2. Interactions of Mes-Y105 with lipid monolayers

Mes-Y105 injected under preformed lipid monolayers at a constant lateral pressure (Π_0) can induce a relative film expansion ($\Delta S/S$). Different behaviors are observed according to the lipid composition of the monolayer (DMPC or DPPG), the initial lateral pressure (15 or 30 mN/m) and the ionic conditions in the subphase, either pH 7.5 with 20 mM Tris buffer or pH 5.5 in pure water. When Mes-Y105 is injected under a DMPC monolayer at pH=7.5, whatever the initial lateral pressure, no $\Delta S/S$ is detected in the Mes-Y105 concentration range from tens of nanomolar up to 1.5 μM (data not shown). When Mes-Y105 is injected under a DPPG monolayer, a significant surface increase is observed whatever the pH even at a high pressure of 30 mN/m (Fig. 6). This means that Mes-Y105 inserts into the packed monolayer and expands the lipid film. The slope of the $\Delta S/S$ curve at pH=5.5 is approximately 1.7 greater than that at pH=7.5, which means a greater expansion of the packed monolayer at low pH. This could be due to more peptide bound and/or to a different molecular area of Mes-Y105 at the interface.

3.2.3. Structure of Mes-Y105 bound to lipids by PMIRRAS

PMIRRAS spectra are registered after injecting Mes-Y105 in the subphase under pre-formed lipid monolayers; different spectra are obtained according to the phospholipid used. The pure lipid spectra were used as standards; they show the bands around 1730, 1460 and 1225 cm^{-1}, respectively, due to ν(C=O) ester, $\delta(CH_2)$ of the acyl chains and $\nu_{as}(PO_2^-)$ of the phosphate group [35].

When Mes-Y105 is injected in the subphase of a DMPC monolayer compressed at 30 mN/m, only pure lipid spectra are detected, even on increasing the peptide concentration up to 1.5 μM (Fig. 7). In contrast, in the presence of the magainin analogue and melittin in the subphase, the peptide vibration bands are readily detected superimposed to those of the lipids (data not shown).

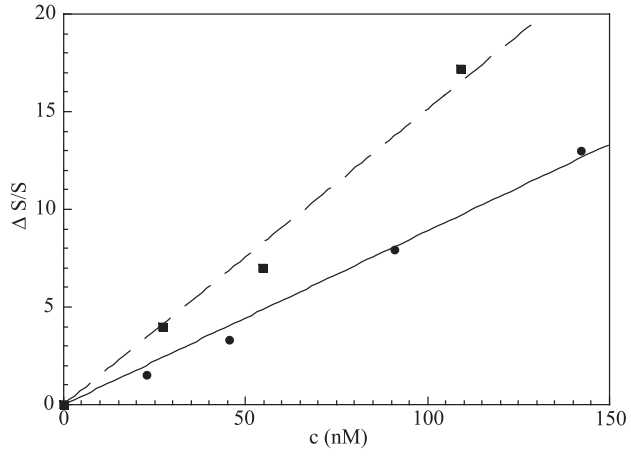

Fig. 6. Relative film surface increases due to Mes-Y105 insertion at Π=30 mN/m in preformed DPPG monolayers on increasing its bulk concentration in the subphase (T=25 °C). (–■–) Subphase: pure water, pH=5.5. (–●–) Subphase: 20 mM Tris buffer, HCl, pH=7.5.

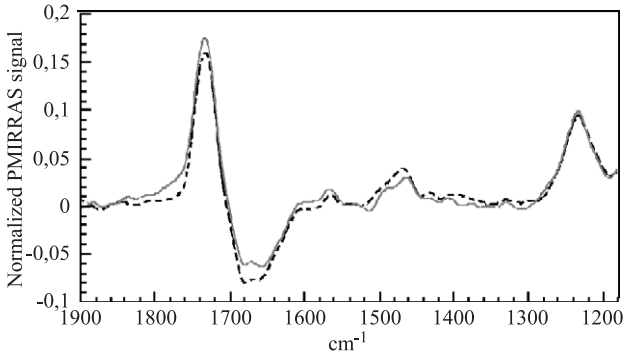

Fig. 7. PMIRRAS spectra of Mes-Y105 in interaction with a DMPC monolayer Π= 30 mN/m. (……) DMPC monolayer; (—) mixed Mes-Y105/DMPC monolayer. Subphase: Tris buffer 20 mM, HCl, pH=7.5; T=23 °C.

Conversely, the PMIRRAS spectra of mixed Mes-Y105/DPPG monolayers compared to pure DPPG in different pH subphase conditions (7.5 and 5.5) show the presence of the peptide due to the amide band contributions (Fig. 8) after Mes-Y105 injection under the DPPG monolayer compressed at 30 mN/m to mimic the lateral pressure in a natural membrane. Moreover, at pH=7.5 there is only a perturbation on the band characteristic of the lipids phosphate heads while there is a broadening of the ν(C=O) ester band and an increase of the $\nu(PO_2^-)$ intensity at pH=5.5 (Fig. 8). These changes traduce a reorientation of the phosphate group and the formation of hydrogen bonds, respectively, both consecutive to Mes-Y105 interaction with the monolayer. At both pHs there is no detectable and significant changes in the $\nu(CH_2)_{as,s}$ bands of the lipid acyl chains (data not shown).

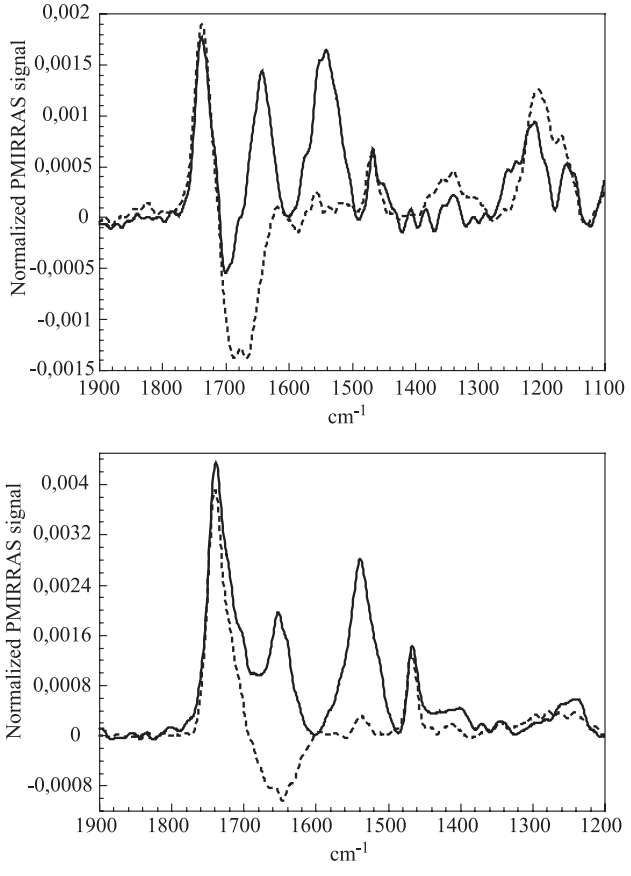

Fig. 8. PMIRRAS spectra of Mes-Y105 in interaction with DPPG monolayers (Π= 30 mN/m) on various pH subphase conditions. Top: pH=7.5: (……) DPPG monolayer, Π= 30 mN/m. (—) Mixed Mes-Y105/DPPG monolayer, Π= 30 mN/m. Tris 20mM buffer subphase, HCl. Bottom: pH=5.5: (……) DPPG monolayer, Π= 30 mN/m. (—) Mixed Mes-Y105/DPPG monolayer, Π= 30mN/m. Subphase: pure water. [Mes-Y105]$_{subphase}$=142 nM.

Fig. 9 displays the subtracted spectra of Mes-Y105 according to the subphase composition, pH and ionic strength. At both pHs (7.5, 20 mM Tris buffer and pH=5.5, pure water), there is a very intense, well-defined and centered at about 1653 cm^{-1} amide I contribution, with shoulders at 1625/1685 cm^{-1} which is characteristic of mainly α-helix with antiparallel β-sheets contribution. The amide I/amide II intensity ratio (1.7 at pH=7.5, and 1.2 at pH=5.5) and the favored β-sheet amide I contribution at 1685 cm^{-1} compared to that at 1625 cm^{-1} would suggest a tilt (≈50°) both of the α-helix axis compared to the interface plane and of the β-sheets, the direction of the β-strands remaining in the interface plane [38].

Then, whatever the pH there is a strong adsorption of the peptide under the compressed DPPG monolayer and it folds onto a well-defined and oriented structure.

3.2.4. BAM study of the morphology of mixed Mes-Y105/DPPG monolayers

The BAM images of a pure DPPG monolayer at 30 mN/m (Fig. 10a and c) differ according to the subphase pH. At pH=5.5, the lipid monolayer is in a homogeneous liquid condensed phase while on pH=7.5 Tris 20 mM subphase, heterogeneities characterize a two-phase system with the coexistence of lipids in a liquid condensed phase (contrasted zone) and lipids in a liquid expanded phase (dark zone).

When Mes-Y105 is injected into the subphase (Fig. 10b and d), the average normalized gray level, then the

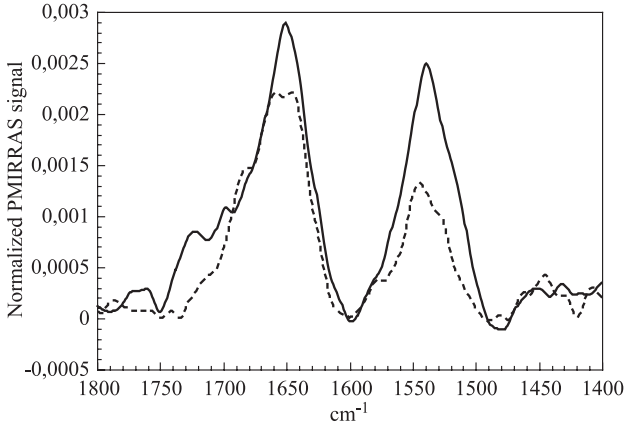

Fig. 9. Subtracted PMIRRAS spectra of mixed Mes-Y105/DPPG monolayers from pure DPPG monolayers (Π=30 mN/m). (—) Pure water subphase, pH=5.5. (---) Tris buffer 20 mM, HCl, pH=7.5. [Mes-Y105]$_{subphase}$=142 nM.

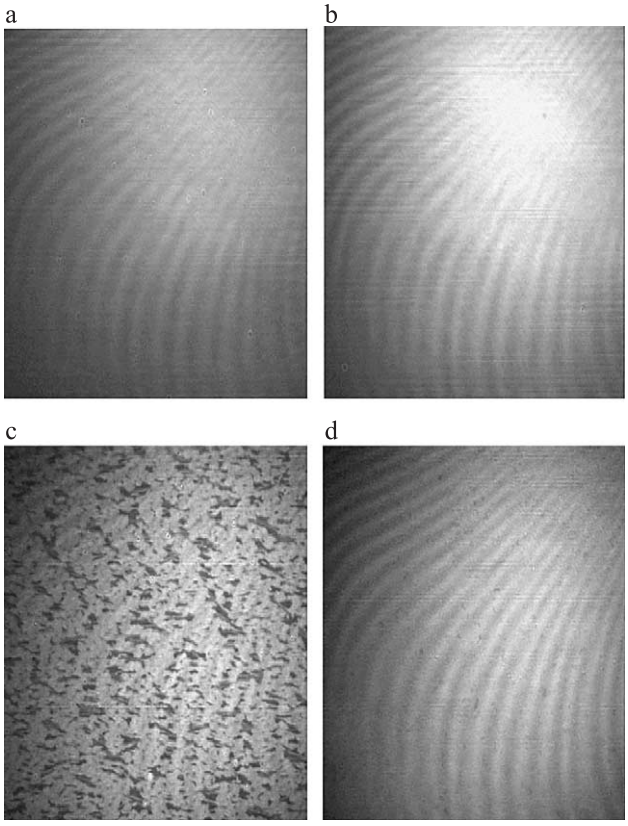

Fig. 10. BAM images of pure DPPG and mixed Mes-Y105/DPPG monolayers (Π=30 mN/m). Top: On pure water subphase, pH=5.5. (a) pure DPPG (GL=100; OS=120); (b) mixed Mes-Y105/DPPG (GL=191; OS=500). Bottom: On tris buffer 20 mM, HCl, pH=7.5. (c) Pure DPPG (GL=91; OS=120); (d) mixed Mes-Y105/DPPG (GL=134; OS=1000). $[\text{Mes-Y105}]_{\text{subphase}}$=142 nM; GL=gray level; OS=obturation speed.

luminosity, strongly increases from 91 up to 1115 and from 100 up to 795 for the pH=5.5 and pH=7.5 subphases, respectively. Such luminosity changes are characteristic both of average thickness and refractive index increases at the interface consecutive to Mes-Y105 adsorption. Furthermore, on pH=7.5 subphase, change in the morphology of the monolayer is observed: the lipid phase transition disappears and the final state displays a homogenous phase of very high brightness.

Using the BAM software, a refractive index of 1.47 for the pure lipid and 1.50 for the mesentericin, it is possible to estimate the thickness of the layers. Then ≈26 Å is obtained for the monolayer of pure DPPG at 30 mN/m, while ≈60 and ≈70 Å are obtained for the mixed Mes-Y105/DPPG monolayers at pH=7.5 and 5.5, respectively.

4. Discussion and conclusions

Previous investigations into class IIa bacteriocins display some predictions of their structure. The N-terminus of these peptides is believed to contain β-sheets maintained in a β-hairpin conformation stabilized by an N-terminal disulfide bridge, while the C-terminal half has been predicted to adopt an amphiphilic α-helix [1,8,9]. In a previous work, we demonstrated using CD spectroscopy in lipid micelles and vesicles that Mes-Y105 displays both α-helix and β-sheet structure [5,39].

Here, we present the first more systematic study relative to the structure of Mes-Y105 in the presence of phospholipids. Our new data will be discussed in four steps, relevant to the putative mode of action of Mes-Y105 on membranes. First, lipid selectivity and affinities will be discussed from approaches using vesicles and monolayers. Then the lipid-induced perturbations will be presented before discussing the secondary structure and orientations of the bound toxin. Finally, this new information will be used to compare Mes-Y105 with other class IIa bacteriocins and to discuss their antibacterial mode of action.

4.1. Mes-Y105 interactions with phospholipid mono- and bilayers, selectivity, affinities and perturbations induced

When Mes-Y105 is in the presence of charged lipids, PS and PG, all the studied physical parameters indicated that interactions occur in the 100 nM to micromolar concentration range changing both the state of the peptide and that of the lipids whatever they are in mono- or bilayers. In similar conditions, all techniques fail to detect significant amounts of toxin bound to zwitterionic lipids, whether in mono- or bilayers. On PC monolayers the toxin inserts only at low film pressure and on vesicles only very high lipid to peptide ratios allow the detection of weak W fluorescence changes and make it possible to estimate an affinity. Moreover, no leakage of fluorescent dye from PC vesicles was detected up to very high peptide concentrations. Therefore, Mes-Y105 selectively interacts with negatively charged lipids as quantitatively indicated by the up to 10^2 factor in the affinity constants found by fluorescence for PG compared to PC. The lipid affinities obtained for PG, from a few to 28 μM (Table 1), compare quite well with the estimated values for pediocin PA-1 (≈39 μM) for DMPG and the total lipids from *Listeria* [7]. The large fluorescence blue shifts observed for W18 and W37 imply that after electrostatic interactions which allow charge compensation at the interface, these residues became strongly dehydrated probably at the lipid interface. A hydrophobic effect is then superimposed onto the dominant electrostatic term. This fits totally with the similar findings on pediocin PA-1 with W residues at positions 18 and 32 [6]. This selectivity of charged lipids in Mes-Y105 fits the general picture for antibacterial peptides as first proposed by Matsuzaki [13,14].

The high binding sensitivity to even low ionic strength and the fairly easy dissociation of complexes by moderate ionic strength (Fig. 3) clearly confirm that affinity is dominated by the electrostatic term. The hydrophobic effect is thus not sufficient to maintain an irreversible binding, and this indicates a lack of deep embedding of the peptide within

the lipids. This is in agreement with the behavior of Mes-Y105 on reversed HPLC, it elutes at RT shorter than magainin, and with the rather low total hydrophobicity, Hi=−2.85, Mes-Y105 is very probably only adsorbed at such a lipid interface with a few non-polar residues at the lipid chains contact. The sevenfold decrease of the affinity in the presence of modest ionic strength (150 mM) is similar to those already found for other toxins like myotoxin or cardiotoxins [20,40,41]. In such cases the binding to lipids was also strictly lipid charge-dependent.

The twofold increase of the lipid affinity observed on decreasing pH from 7.5 to 5.5 (Table 1) as well as the 1.7 factor of expansion of compressed DPPG monolayers at pH 5.5 compared to pH 7.5 result from the increased net positive charge of the peptide due to the protonation of H residue and NH_2 terminal, as well as probably the partial protonation of the E_{20} carboxylate groups of which pK values at interface could be significantly increased [42].

The Mes-Y105 analogues qualitatively behave quite similarly to the parent peptide. Mes-Y105/W18 has affinities similar to Mes-Y105 (Table 1) but the lipid selectivity of Mes-Y105/W37 varies: the affinity for PC increases while that for PS decreases threefold resulting only in a twofold higher affinity for PS compared to PC. Such a change was not anticipated and cannot be accounted for by the difference in hydrophobicity of the two residues as usually defined [43] but probably reflects the peculiar ability of W_{37} to settle at the lipid interface [41,44]. The lower specificity of Mes-Y105/W37 has to be paralleled with the well-established requirement of W_{37} for cytolytic activity [5]. Therefore, in further studies, it would be necessary to check the consequences on antimicrobial activity of F to W replacement at position W37.

The lack of any significant lipid perturbation and $\Delta S/S$ increase on DMPC monolayers, as well as the lack of any dye escape from PC vesicles, only reflects the lack of interaction of Mes-Y105 with the zwitterionic lipids. The perturbations resulting from peptide interactions with PG systems are first detected at the mesoscopic level from BAM pictures, indicating probably changes in the phase stability as already documented for lipid–protein interactions dominated by electrostatics [45,46]. From IRFT no effect is detected on the acyl chains vibrations, while changes in the polar groups are seen on the phosphate and carbonyl vibration bands. The fact that lipid perturbation remains localized at the interface is coherent with a very limited insertion of the peptide which essentially caps the lipids.

4.2. Mesentericin secondary structure and orientation when phospholipid-bound

As soon as the charges induce the proper positioning of Mes-Y105 at interface, the weak total hydrophobicity is not sufficient to allow an insertion into the lipids, especially at high pressures which are relevant for biological membranes. However, the proposed structure with folding of Mes-Y105 17–31 segment into an amphipathic α-helix [5] allows the recovery of a 15-residue-long fragment which has a high hydrophobic moment, μ_H=4.64, i.e., $(\mu_H)_{res}$=0.310, i.e., highly comparable to that of other less specific antibacterial α helical peptides, $(\mu_H)_{res}$=0.286 for magainin. The PMIRRAS data and the fluorescence conclusions indicate that this structure could be extended to the CO terminal where the W37 role should be to "lock" that fragment at the lipid interface. The contributions from FW will indeed increase the total hydrophobic stabilizing effect.

Such a structure agrees to some extent with what has been proposed for Mes-Y105 by CD in solution [5] and also documented in the presence of lysoPC micelles and DMPG vesicles [39]. High resolution NMR on Leucocin A and carnobacteriocin B [8,9] also agree with our data even though such studies were performed in very different conditions (very high peptide concentrations bound to detergent micelles of lyso zwitterionic PC at very extreme pH 2 value). Our proposal that the CO-terminal is involved at the membrane interface could allow a lengthening of the α-helix up to 20 residues. Indeed, even if the presence of three G residues could destabilize helices in solution, it was demonstrated to be compatible with such a folding at the membrane interface [47]. IRFT and CD data are compatible with such a model, but since their accuracy has reached its limit it is not possible to certify this assumption. Mes-Y105 has a peculiar charge distribution: at pH 7.5 the amphipathic helix has no net charge, the net cationic charge being only due to the β-sheeted N-terminal segment. On the contrary, at low pH the amphipathic helix acquires a positive charge becoming therefore more similar to the antibacterial units of the classic antibacterial peptides. Concomitantly, the net charge on the N-terminal segment increases and results in an increased affinity for charged lipids as soon as these species remain strongly negative. This was shown for PG lipids present in bacterial membranes and especially in *Listeria*, for LPS and sulfatides present in other bacterial membranes but not for PS or any other carboxylate containing lipids which also can have a decreased net lipid charge at low pH [6,7,7–48].

The limited insertion of Mes-Y105 in the DPPG and its tilted orientation ($\approx 50^\circ$ towards the interface plane) determined by PMIRRAS are coherent with the thickness estimation obtained by BAM. Since no reorientation of chains was observed by PMIRRAS, the lipid thickness does not change drastically after Mes-Y105 interaction, then a Mes-Y105 layer of 34 to 44 Å is formed at the interface. This thickness is compatible neither with that of a flat α-helix at the interface plane (<16 Å) nor with a flat and short β-sheet. The structure and orientation of Mes-Y105 are similar at both pH (5.5 and 7.5) then the thicker layer obtained at pH=5.5 is due to more peptide bound to the lipid monolayer, which agrees with the higher affinity for the negatively charged interface of +4 charged Mes-Y105 at pH=5.5 compared to the +2 Mes-Y105 at pH=7.5.

4.3. Comparison with other class IIa bacteriocins

The interactions documented herein with PG lipids can be relevant for the mode of action of Mes-Y105 since target cells, for example *Listeria* membranes, are PG-rich [6]. However, the cytotoxic selectivity could require binding to other charged lipids since the affinities documented here are not high enough and/or, more importantly, are too sensitive to ionic strength or the membrane counter ions. Indeed, more structural data are required to ensure a definitive model for Mes-Y105 bound onto the membrane and to define the exact role of each one of the three structural motifs (N-terminal β-sheet, amphipathic α-helix, C terminal domain [9]). The proposal for a new role of the C terminal has to be checked. Conversely, looking at Y residues of Mes-Y105 could generate more direct information on the involvement of the N-terminal fragment at the contact of lipid negatively charged groups. This could shed some light on the need or not for a specific toxin receptor. Finally, these conclusions of electrostatically dominated binding to some specific lipid could be sufficient to explain the differences of affinities and mic's values of the other class II bacteriocins, especially their pH toxicity dependence [6]. On the other hand, with knowledge of many bacteriocin sequences [1], our study shows that W fluorescence can be used systematically to monitor interactions, classify their lipid affinities and to attempt to correlate them with their cytotoxic activities. As W18 is almost invariant in the sequences, it would be a good and sensitive reporter. One can anticipate that for toxins having a single W18 residue like carnobacteriocin B2 and bavaricin A [1], the intrinsic fluorescence should behave similarly to Mes-Y105/W18. In contrast, as Mes-Y105 and Leucocin A are the shorter members of that bacteriocin family, it would also be interesting to look, using single mutation like herein Mes-Y105/W18, at the behavior of the other bacteriocins' last W which is often in position close to 37, but not at the C-terminal of the toxins. This could differentiate the relative roles of the W anchor and the C-terminal charge of the toxins more definitively.

References

[1] S. Ennahar, T. Sashihara, K. Sonomoto, A. Ishizaki, Class IIa bacteriocin: biosynthesis, structure and activity, FEMS Microbiol. Rev. 24 (2000) 85–106.

[2] C. Fremeaux, Y. Héchard, Y. Cenatiempo, Mesentericin Y105 gene clusters in *Leuconostoc mesenteroides* Y105, Microbiology 141 (1995) 1637–1645.

[3] Y. Héchard, B. Dérijard, F. Letellier, Y. Cenatiempo, Characterization and purification of mesentericin Y105, an anti-*Listeria* bacteriocin from *Leuconstoc mesenteroides*, J. Gen. Microbiol. 138 (1992) 2725–2731.

[4] A. Maftah, D. Renault, C. Vignoles, Y. Héchard, P. Bressolier, M.H. Ratinaud, Y. Cenatiempo, R. Julien, Membrane permeabilization of *Listeria monocytogenes* and mitochondria by bacteriocin mesentericin Y105, J. Bacteriol. 175 (1993) 3232–3235.

[5] Y. Fleury, M.A. Dayem, J.J. Montagne, E. Chamboiseau, J.P. Le Caer, P. Nicolas, A. Delfour, Covalent structure, synthesis and structure–function studies of Mesentericin Y105, a defensive peptide from gram-positive bacteria, J. Biol. Chem. 271 (1996) 14421–14429.

[6] Y. Chen, R.D. Ludescher, T.J. Montville, Electrostatic interactions, but not the YGNGV consensus motif, govern the binding of pediocin PA-1 and its fragments to phospholipid vesicles, Appl. Environ. Microbiol. 63 (1997) 4770–4777.

[7] Y. Chen, R.D. Ludescher, T.J. Montville, Influence of lipid composition on pediocin PA-1 binding to phospholipid vesicles, Appl. Environ. Microbiol. 64 (1998) 3530–3532.

[8] N.L. Fregeau-Gallacher, M. Sailer, W.P. Niemczura, T.T. Nakashima, M.E. Stiles, J.C. Verderas, Three-dimensional structure of Leucocin A in TFE and dodecylphosphocholine micelles: spatial location of residues critical for biological activity in type IIa bacteriocins from lactic acid bacteria, Biochemistry 36 (1997) 15062–15072.

[9] Y. Wang, M.E. Henz, N.L. Fregeau-Gallacher, S. Chai, A.C. Gibbs, L.Z. Yan, M.E. Stiles, D.S. Wishart, J.C. Vederas, Solution structure of Carnobactericin B2 and its implication for structure-activity relationships among type IIa bacteriocins from lactic acid bacteria, Biochemistry 38 (1999) 15438–15447.

[10] C. Corbier, F. Krier, G. Mulliert, B. Vitoux, A.M. Revol-Junelles, Biological activities and structural properties of the atypical bacteriocins mesenterocin 52B and leucocin B-TA-33a, Appl. Environ. Microbiol. 67 (2001) 1418–1422.

[11] P. Nicolas, A. Mor, Peptides as weapons against microorganisms in the chemical defense system of vertebrates, Annu. Rev. Microbiol. 49 (1995) 277–304.

[12] B. Bechinger, The structure, dynamics and orientation of antimicrobial peptides in membranes by multidimensional solid-state NMR, Biochim. Biophys. Acta 1462 (1999) 157–183.

[13] K. Matsuzaki, Why and how peptide–lipid interactions utilized for self-defense? Magainins and tachyplesins as archetypes, Biochim. Biophys. Acta 1462 (1999) 1–10.

[14] Y. Shai, Mechanism of binding, insertion and destabilization of phospholipid bilayer membranes by antibacterial and cell non-selective membrane lytic peptides, Biochim. Biophys. Acta 1462 (1999) 55–70.

[15] D. Blaudez, J.M. Turlet, J. Dufourcq, D. Bard, T. Buffeteau, B. Desbat, Investigations at the air/water interface using polarization modulation IR spectroscopy, J. Chem. Soc., Faraday Trans. 92 (1996) 525–530.

[16] G.B. Fields, R.L. Noble, Solid phase peptide synthesis utilizing 9-fluorenylmethoxycarbonyl amino acids, Int. J. Pept. Protein Res. 35 (1990) 161–214.

[17] D.S. King, C.G. Fields, G.B. Fields, A cleavage method which minimizes side reactions following Fmoc solid phase peptide synthesis, Int. J. Pept. Protein Res. 36 (1990) 255–266.

[18] E. Thiaudière, Thèse Université Bordeaux I (1990).

[19] E. Perez-Paya, J. Dufourcq, L. Braco, C. Abad, Structural characterisation of the natural membrane bound state of melittin: a fluorescence study of a dansylated analogue, Biochim. Biophys. Acta 1323 (1997) 223–236.

[20] J. Dufourcq, F. Dousseau, J.F. Faucon, A.T. Tu, Myotoxin a-phospholipid interactions, an attempt by intrinsic fluorescence to define a possible mode of action for the toxin on membranes, Appl. Spectrosc. 41 (1987) 1410–1417.

[21] W.K. Surewicz, R.M. Epand, Role of peptide structure in lipid–peptide interactions: a fluorescence study of the binding of pentagastrin-related pentapeptides to phospholipid vesicles, Biochemistry 23 (1984) 6072–6077.

[22] S. Castano, B. Desbat, M. Laguerre, J. Dufourcq, Sructure, orientation and affinity for interfaces and lipids of ideally amphipathic lytic $L_iK_j(i{=}2j)$ peptides, Biochim. Biophys. Acta 1416 (1999) 176–194.

[23] D. Blaudez, T. Buffeteau, J.C. Cornut, B. Desbat, N. Escafre, M. Pezolet, J.M. Turlet, Polarization modulation IRFT spectroscopy at the air–water interface, Thin Solid Films 242 (1994) 146–150.

[24] J. Dufourcq, J.F. Faucon, R. Maget-Dana, M.P. Pileni, C. Helene, Peptide–membrane interactions: a fluorescence study of the binding of di- and tri-peptide containing Lys and Tyr or Trp residues to phospholipid vesicles, Biochim. Biophys. Acta 649 (1981) 67–76.
[25] W.F. De Grado, F.J. Kézdy, E.T. Kaiser, Design, synthesis, and characterization of a cytotoxic peptide with melittin-like activity, J. Am. Chem. Soc. 103 (1981) 679–681.
[26] S. Castano, I. Cornut, K. Büttner, J.L. Dasseux, J. Dufourcq, The amphipathic helix concept: length effects on ideally amphipathic L_iK_j(i=2j) peptides to acquire optimal hemolytic activity, Biochim. Biophys. Acta 1416 (1999) 161–175.
[27] E. Perez-Paya, J. Dufourcq, L. Braco, C. Abad, Structural characterization of the natural membrane-bound state of melittin: a fluorescence study of a dansylated analogue, Biochim. Biophys. Acta 1329 (1997) 223–236.
[28] K. Matsuzaki, M. Harada, S. Funakoshi, N. Fujii, K. Miyajima, Physicochemical determinants for the interactions of magainins 1 and 2 with acidic lipid bilayers, Biochim. Biophys. Acta 1063 (1991) 162–170.
[29] K. Matsuzaki, O. Murase, H. Tokuda, S. Funakoshi, N. Fujii, K. Miyajima, Orientational and aggregational states of magainin 2 in phospholipid bilayers, Biochemistry 33 (1994) 3342–3349.
[30] T.E. Creighton, Proteins, Structure and Molecular Properties, W.H. Freeman and Company, New York, 1996.
[31] T. Miyazawa, Infrared Spectra and Helical Conformations, Marcel Dekker, New York, 1967.
[32] P.I. Haris, D. Chapman, Does Fourier-transform infrared spectroscopy provide useful information on protein structure? TIBS 17 (1992) 328–333.
[33] W.K. Surewicz, H.H. Mantsch, D. Chapman, Determination of protein secondary structure by Fourier transform infrared spectroscopy: a critical assessment, Biochemistry 32 (1993) 389–394.
[34] E. Goormaghtigh, V. Cabiaux, J.M. Ruysschaert, Determination of soluble and membrane protein structure by Fourier transform infrared spectroscopy: assignments and model compounds, in: H.J. Hilderson, G.B. Ralston (Eds.), Subcellular Biochemistry: Physicochemical Methods in the Study of Biomembranes, Plenum Press, New York, 1994, pp. 329–362.
[35] I. Cornut, B. Desbat, J.M. Turlet, J. Dufourcq, In situ study by polarization modulated Fourier transform infrared spectroscopy of the structure and orientation of lipids and amphipathic peptides at the air/water interface, Biophys. J. 70 (1996) 305–312.
[36] S. Castano, B. Desbat, J. Dufourcq, Ideally amphipathic β-sheeted peptides at interfaces : structure, orientation, affinities for lipids and hemolytic activity of $(KL)_mK$ peptides, Biochim. Biophys. Acta 1463 (2000) 65–80.
[37] P. Bhugaloo-Vial, X. Dousset, A. Metivier, O. Sorokine, P. Anglade, P. Boyaval, D. Marion, Purification and amino-acid sequences of piscicocins V1a and V1B, two class IIa bacteriocins secreted by *Carnobacterium piscicola* V1 that display significantly different levels of specific inhibitory activity, Appl. Environ. Microbiol. 62 (1996) 4410–4416.
[38] T. Buffeteau, E. Le Calvez, S. Castano, B. Desbat, D. Blaudez, J. Dufourcq, Anisotropic optical constant of α-helix and β-sheet secondary structures in the infrared, J. Phys. Chem., B 104 (2000) 4537–4544.
[39] S. Castano, B. Desbat, A. Delfour, J.M. Dumas, F. Aussenac, A. Da Silva, J. Dufourcq, Lipid-bound structure and phospholipid selectivity of Mesentericin Y105, a bacteriocin from *Leuconostoc mesenteroïdes* and Trp substituted analogues, Peptides 2002—Proc. 27th Eur. Peptides Soc., Sorrento, 2002, pp. 738–739.
[40] J. Dufourcq, J.F. Faucon, Specific binding of a cardiotoxin from *Naja mossambica mossambica* to charged phopholipids detected by intrinsic fluorescence, Biochemistry 17 (1978) 1770–1776.
[41] F. Dousseau, J.F. Faucon, J. Dufourcq, in: K.L. Mittal, P. Bothorel (Eds.), 5th International Symposium on Surfactants in Solution, Plenum Press, New York, 1986, pp. 907–916.
[42] M. Ptak, M. Egret-Charlier, A. Sanson, O. Bouloussa, A NMR study of the ionization of fatty acids, fatty amines and *N*-acylamino acids incorporated in phosphatidylcholine vesicles, Biochim. Biophys. Acta 600 (1980) 387–397.
[43] D. Eisenberg, R.M. Weiss, T.C. Terwilliger, The helical hydrophobic moment: a measure of the amphiphilicity of α helix, Nature 299 (1982) 371–374.
[44] S.H. White, W.C. Wimley, A.S. Ladokhin, K. Hristova, Protein folding in membranes: determinating the energetics of peptide–bilayers interactions, Methods Enzymol. 295B (1998) 62–87.
[45] J.F. Faucon, J. Dufourcq, E. Bernard, L. Ducheneau, M. Pézolet, Abolition of the thermotropic transition of charged phospholipids induced by a cardiotoxin from *Naja mossambica mossambica* as detected by fluorescence polarization, differential scanning calorimetry and Raman spectroscopy, Biochemistry 22 (1983) 2180–2185.
[46] E. Bernard, J.F. Faucon, J. Dufourcq, Phase separations induced by melittin in negatively charged phospholipid bilayers as detected by fluorescence polarization and differential scanning calorimetry, Biochim. Biophys. Acta 688 (1982) 152–162.
[47] S.C. Li, C.M. Deber, Glycine and beta-branched residues support and modulate peptide helicity in membrane environments, FEBS Lett. 311 (1992) 217–220.
[48] Y. Chen, R. Shapira, M. Eisenstein, T. Montville, Functional characterization of pediocin PA-1 binding to liposomes in the absence of a protein receptor and its relationship to a predicted tertiary structure, Appl. Environ. Microbiol. 63 (1997) 524–531.